Interactions between Polymer-Coated Surfaces in Poor Solvents. 1. Surfaces Grafted with A and B Homopolymers

Chandralekha Singh,[†,‡] Galen T. Pickett,[†] and Anna C. Balazs[*,†]

Department of Chemical and Petroleum Engineering, Physics and Astronomy Department, University of Pittsburgh, Pittsburgh, Pennsylvania 15261

Received June 4, 1996[⊗]

ABSTRACT: Using a two-dimensional self-consistent field theory, we investigate the interaction between two planar surfaces where (1) each surface is grafted with both A and B homopolymers and (2) one surface is coated with end-grafted A's and the other is coated with end-grafted B's. The chains are grafted at low densities and the B polymers are chosen to be solvophobic. We vary the solvent affinity of the A chains and the interaction between the A and B monomers. We determine the morphology of the layers and the energy of interaction as the layers are compressed. The energy of interaction versus distance profiles show a wide region of attraction as the surfaces are brought together. This attractive interaction is due to the self-assembled structures that appear at low grafting densities in poor solvents. The properties of the attraction can be tailored, as we demonstrate in a simple scaling picture. Our findings indicate that fine control over the pair interaction function of coated colloidal particles can be gained through grafting mixtures of homopolymers.

Introduction

The properties of a suspension of particles can be tailored by tethering polymer chains to the particles. The effect of the chains can be controlled by varying the solvent quality. In a good solvent, the tethered chains extend into the solution and sterically stabilize the suspension. In a poor solvent, the tethered chains collapsed and the particles flocculate. A detailed understanding of the pair interactions mediated by the tethered polymers permits the rational design of optimal coatings. While the forces between polymer-coated surfaces in good solvents have undergone close scrutiny,[1−6] the interactions between polymer layers in poor solvents have not been extensively investigated.[7−9] Thus, our understanding of these poor-solvent interactions is incomplete.

Recently, we used a two-dimensional self-consistent field (SCF) theory to examine the energy of interaction between two planar surfaces that are sparsely coated with end-grafted homopolymers and immersed in a poor solvent.[8] The layers experience an attraction as they are brought together, in contrast to the repulsive interaction that is observed when the layers are compressed in a good solvent. In addition, through the 2D SCF, we could characterize the laterally inhomogeneous structures that are formed as the separation between the surfaces is decreased. At large surface separations, each layer forms "pinned micelles".[10−13] When the surfaces are compressed, attraction between the layers causes the micelles from the two surfaces to merge, forming a larger micelle or "bundle", which can extend from one surface to the other.

In the above study, the surfaces were coated with a single species of homopolymer. In this paper, we consider how the interaction between the surfaces can be tailored by grafting two distinct types of homopolymers. In particular, we use the 2D SCF model to calculate the energy of interaction and the morphology of the layer when A and B homopolymers are end-grafted to the surfaces and the layers are brought into contact. In part 2 of this study, we examine the interaction between surfaces that are covered with AB diblock copolymers. In both studies, the chains are grafted at relatively low densities and at least one of the homopolymers or blocks is in a poor solvent. Here, we focus on the two classes of systems shown schematically in Figure 1: (a) each surface is covered with grafted A and B chains and (b) one surface is coated with homopolymer A and the other is coated with homopolymer B. We investigate the behavior of the system as a function of the relative polymer−solvent interactions, the polymer−polymer interactions, and chain length.

We emphasize that our calculations are restricted to the case of low grafting densities, where the formation of pinned micelles is most pronounced.[13] As will be seen below, these structures have a dramatic influence on the interaction between the surfaces and yield results that are in contrast to the case of high grafting densities.[14] For example, Chen et al.[7] used a one-dimensional SCF theory to examine the high density case for grafted A and B chains, where one homopolymer is solvophobic and the other is solvophilic. They find a monotonic repulsion between the grafting surfaces. However, using a two-dimensional SCF theory for the low density case, we find a wide region of attraction as the surfaces are brought together. This attractive interaction is due to the self-assembled structures that appear at low grafting densities in poor solvents.

These structures are inherently three-dimensional, so we must allow variations in at least two dimensions in our numerical calculations to capture the important lateral inhomogeneities. As described below, our SCF calculations thus only qualitatively reflect the true three-dimensional system. We further analyze this three-dimensional system with a simple scaling argument and verify that our SCF results are qualitatively correct.

The SCF Model

The SCF calculations provide a description of the system at thermodynamic equilibrium. One-dimensional SCF theory, however, is insufficient for describing the structure of laterally inhomogeneous structures such

* Author to whom correspondence should be addressed.
† Department of Chemical and Petroleum Engineering.
‡ Physics and Astronomy Department.
⊗ Abstract published in *Advance ACS Abstracts,* October 1, 1996.

S0024-9297(96)00812-1 CCC: $12.00

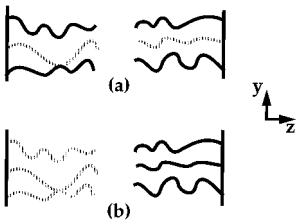

Figure 1. Schematic diagram of two end-grafted brushes (a) with alternately grafted A−B chains and (b) with surfaces coated with homopolymers of different solvent qualities.

as pinned micelles. We therefore use a two-dimensional SCF theory, which is a generalization of the 1D model developed by Scheutjens and Fleer.[15] In the Scheutjens and Fleer theory, the phase behavior of polymer systems is modeled by combining Markov chain statistics on a lattice (the mesh size of which is the Kuhn length for both A and B polymers) with a mean field approximation. Since the method is thoroughly described in ref 15, we simply provide the basic equations and refer the reader to that text for a more detailed discussion.

To start, the free energy per lattice site in the mean field approximation is given by

$$f(r) = \sum_{i,c} n_{i,c}(r) \ln n_{i,c}(r) + (1/2)\sum_{j,k}\chi_{j,k}\int \eta(r-r')\,\phi_j(r)\,\phi_k(r')\,dr' \quad (1)$$

where the first term on the right hand side represents the entropy of mixing and the second term is the enthalpic contribution. The parameter $n_{i,c}(r)$ is the number density at r of molecules of type i in conformation c. In the enthalpic term, the indices j and k run over all the different types of monomers and $\phi_j(r)$ represents the average density of monomers j at r. The $\chi_{j,k}$ term is the Flory−Huggins interaction parameter and $\eta(r-r')$ is the short-range interaction function, which can be replaced by a summation over nearest neighbors.

To calculate the segment density distribution $\phi_j(r)$ that minimizes the free energy, we exploit the analogy between the trajectory followed by a diffusing particle and the conformation of a chain.[15] We define Green's functions of the type $G(r_1,N'|r_2,N'')$ as the combined statistical weight of all conformations of a subchain starting with segment N' at r_1 and ending with segment N'' at r_2. For a homopolymer, the set of Green's functions for $N' < N''$ and $N' > N''$ are identical and obey the recursion relation

$$G(r,N'|r_1,1) = \exp[-U_i(r)]\int G(r',N'-1|r_1,1)\,\eta(r-r')\,dr' \quad (2)$$

along with the boundary condition

$$G(r,1|r',1) = \exp[-U_i(r)]\,\delta_{r,r'} \quad (3)$$

where $\delta_{r,r'}$ is the Kronecker delta, and r and r' are the variables that denote the beginning and end of the chain, respectively. The parameter $U_i(r)$ is the potential of mean force acting on segment i at point r and is given by

$$U_i(r) = \alpha(r) + \sum_{k}\chi_{i,k}\int \phi_k(r')\,\eta(r-r')\,dr' \quad (4)$$

where $\alpha(r)$ is a hard core potential that ensures incompressibility. The segment density distribution can be calculated from the Green's functions as

$$\phi_j(r) = \sum_i C_i \exp[-U_j(r)]\sum_{N'\in j}\int G(r,N'|r_1,1)\,G(r,N'|r_2,N_i)\,dr_1\,dr_2 \quad (5)$$

where N_i is the length of molecule i and C_i is the normalization constant, which can be obtained from the total number of molecules, n_i:

$$C_i = n_i/[\sum_{N'}\int G(r_1,N'|r_2,1)\,dr_1\,dr_2] \quad (6)$$

From eqs 2−6, the self-consistent density distribution for the different types of segments can be calculated by discretizing the equations and solving them numerically.[15]

We note that the expression for the excess free energy in terms of segment density distribution is given by

$$F(r) = \sum_j \phi_j(r) \ln G_j(r) + (1/2)\sum_{jk}\chi_{j,k}\int \eta(r-r')\,\phi_j(r)\,\phi_k(r')\,dr' \quad (7)$$

For two grafted layers, the free energy of interaction as a function of surface separation, L, can be obtained by taking the difference between the free energies when the layers are infinitely apart and when they are separated by a distance, L.

In the two-dimensional SCF theory,[16] the above equations are explicitly written in terms of Z and Y, the directions perpendicular and parallel to the grafted layer, respectively. We assume translational invariance along X.

In our 2D SCF calculations, we consider two planar surfaces that lie parallel to each other in the XY plane and investigate the effect of bringing the surfaces closer together in the Z direction. Each surface is covered with monodisperse end-grafted polymers. The ends of the chains are grafted to impenetrable surfaces at $Z = 1$ and $Z = L$.

The grafted polymers are characterized by three sets of parameters: grafting density, chain length, and the relevant χ parameters. We fix the grafting density per line along the Y direction at 0.5 for all calculations; i.e., the polymers are grafted on alternate lattice sites. The grafting density per line along the X direction is denoted by ρ and is fixed at $\rho = 0.025$ for all of the results presented below. (Thus, the average area per chain, s, has $s = 2/\rho$.) We let χ_{AS} and χ_{BS} represent the polymer−solvent interactions for the A and B components, respectively, and χ_{AB} is the interaction parameter for the two different monomers. The strength of interaction between the polymers and the planar, impenetrable surface is assumed to be the same as that between the polymer and the solvent. We fix the polymer−solvent interaction for the B chains at $\chi_{BS} = 2$, while gradually varying χ_{AS} from 0 to 1. We also set $\chi_{AB} = 0$ and subsequently determine the effect of increasing $\chi_{AB} > 0$.

We apply periodic boundary conditions along the Y direction. To ensure the lowest energy configuration and to minimize the boundary effects in poor solvents (when the system forms pinned micelles), we change the lateral dimension, L_y in the Y direction and plot the free energy of the system as a function of L_y. The free energy is a periodic function of L_y and the minima of the free energy corresponds to the values of L_y where an integer

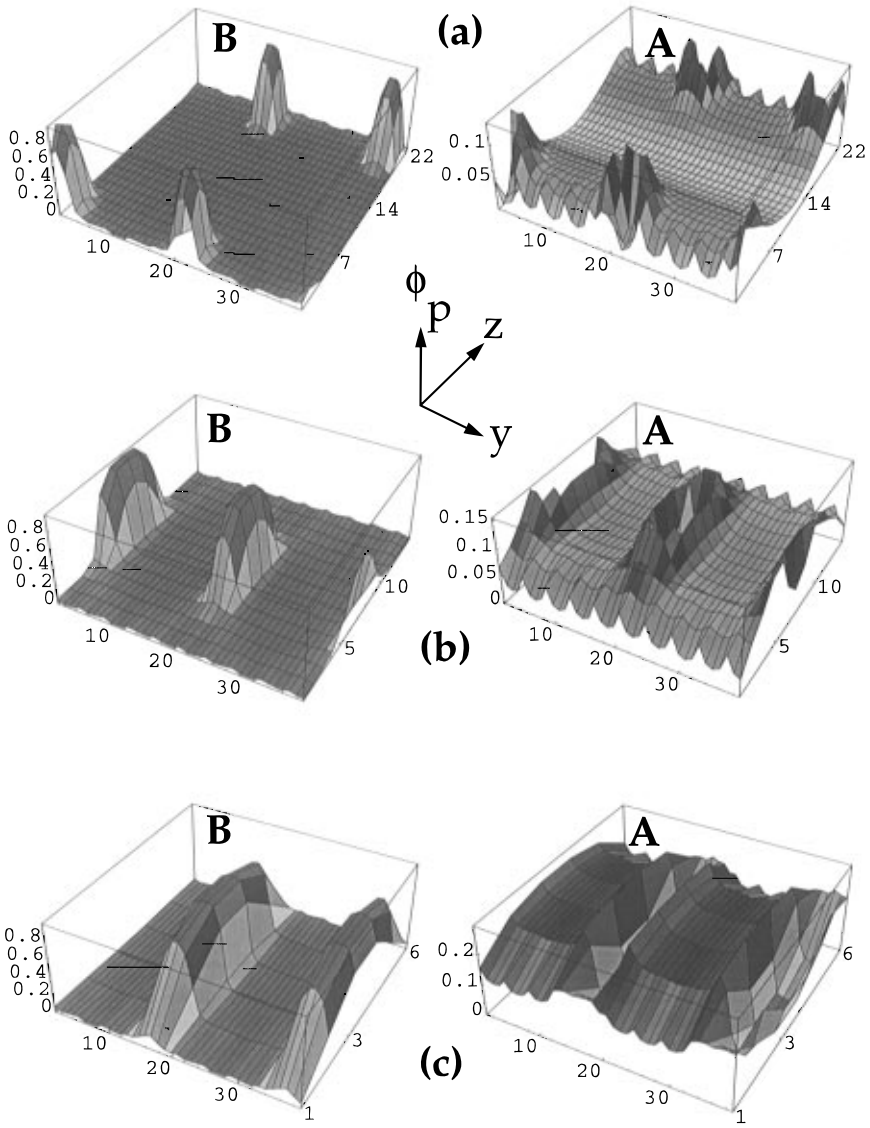

Figure 2. Plots showing the effect of decreasing the surface separation, L, for alternately grafted A−B chains where $N_A = N_B = 80$. The grafting density per line ρ is 0.025, $\chi_{Bs} = 2$, $\chi_{As} = 0$, and $\chi_{AB} = 0$. The figures are for the following surface separations: (a) $L = 21$, (b) $L = 13$, and (c) $L = 5$. Y refers to the grafting direction and ϕ_p denotes the polymer density. The plots marked "B" show the polymer density of the B blocks, while the plots marked "A" show the density of the A blocks.

number of undistorted micelles fit in the box. Calculations are performed for L_y corresponding to one of these minima. For each parameter set, the distance between two consecutive free energy minima determines the distance between two micelles. The size of a micelle and the distance between them is determined by the competition between the stretching energy and the free energy of interaction. Varying the system parameters will, therefore, change the size of the micelles and the distance between them so that L_y is different for each parameter set.

We note that our assumption of translational invariance along the X direction implies that the three−dimensional structures corresponding to our system are rows of long cylindrical micelles pinned at the surfaces. The true three-dimensional structure is expected to have an array of spherical micelles pinned to each surface. Therefore, our SCF calculations indicate general trends and morphologies rather than quantitative predictions.

SCF Results: Interactions and Morphologies

Alternately Grafted A and B Chains of Equal Length. Effect of Varying χ_{AS}; $\chi_{BS} = 2$, $\chi_{AB} = 0$. We consider two surfaces coated with alternately grafted A and B homopolymers, where $N = 80$ for both types of chains. We fix $\chi_{BS} = 2$, $\chi_{AB} = 0$ and initially set $\chi_{AS} = 0$. Figure 2 shows how the self-assembly of the polymers is affected by the compression of the layers. At large surface separations (Figure 2a), the chains form distinct structures on each of the substrates. In particular, the more solvophobic B chains associate into a dense core and the A chains form an outer shell that encircles this region. In this configuration, the B domain is shielded from the unfavorable solvent and the surface tensions within the system are minimized. Since the A chains are in a good solvent, they extend into the solution and their density slowly decays away from the B core. Thus, these surface micelles have a "flower-like" appearance.[17]

As the layers are brought closer together, the B cores from the two surfaces merge to form a single micelle that is situated half way between the two surfaces (Figure 2b). The A chains from both surfaces now form a common shell around the micelle, so that the structure goes from resembling two "flowers" on each of the surfaces to one in the center. It is important to note that the merging of micelles happens at a distance that is significantly greater than the vertical extent of the

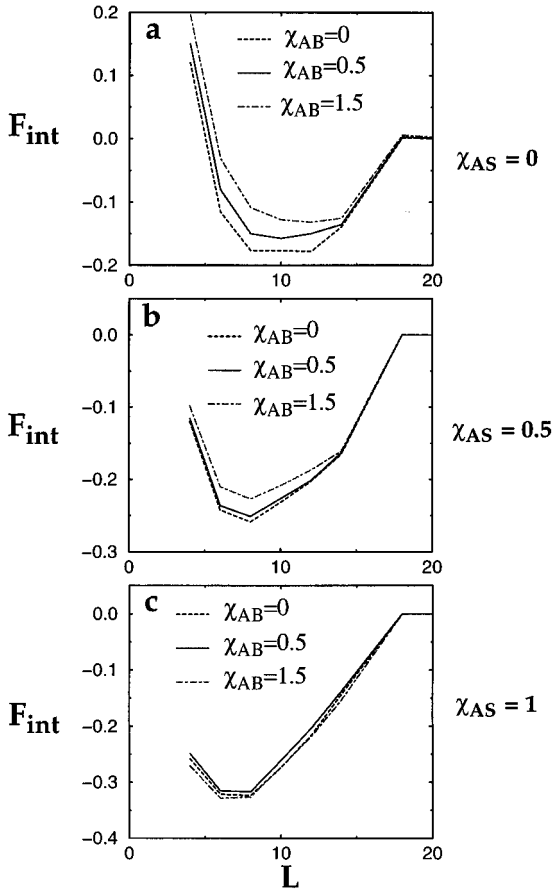

Figure 3. Free energy of interaction per grafted line, F_{int}, as a function of surface separation, L, for alternately grafted A−B chains where $N_A = N_B = 80$. The grafting density per line, ρ, is 0.025 and $\chi_{Bs} = 2$. The A−solvent interaction is (a) $\chi_{As} = 0$, (b) $\chi_{As} = 0.5$, and (c) $\chi_{As} = 1$. Each of the figures shows results for three different χ_{AB}, which are shown with different types of lines.

isolated micelles. In fact, the merging occurs when L is comparable to the lateral spacing of the pinned micelles, consistent with our scaling arguments below. This behavior can be understood by considering the balance between the benefit to increasing the volume of the B core while minimizing its surface area. The merger of the solvophobic cores reduces unfavorable B−solvent contacts. Moreover, the solvophilic A chains now form a common shell that extends farther (and hence has more entropic degrees of freedom) than if it was just shielding the micelle formed by the chains on the same surface.

With further decreases in the surface separation, more and more solvent is expelled from the system and the density of the soluble component around the micellar core increases (Figure 2c). This reduces the B−solvent contacts and leads to further enthalpic gains. We note that the compression of the surfaces and squeezing out of the solvent only affects the density of the soluble component, but leaves the density of the B core more or less unchanged (Figure 2c).

In Figure 3a, we plot the free energy of interaction, F_{int}, as a function of surface separation, L. The interactions are repulsive when $F_{int} > 0$ and attractive when $F_{int} < 0$. (When the surfaces are sufficiently far apart that the layers do not interact, $F_{int} = 0$.) As the surfaces are brought together, the solvophilic A layers (or the "petals" of the flowers) come in contact with each other and the free energy shows a very small repulsion (almost imperceptible in the plot). When the B cores merge, the free energy of interaction begins to decrease (near $L = 18$). As the compression continues, there is a point at which the entropic losses start dominating and the free energy of interaction becomes repulsive.

If we systematically increase χ_{AS} from 0 to 0.5 (representing a Θ solvent for the A component) and then to 1.0 (a poor solvent for A) while keeping $\chi_{BS} = 2$, the qualitative features are similar to those described above. However, the A chains are now less soluble in the surrounding solution and in the case of $\chi_{AS} = 1.0$, are even solvophobic. Thus, the A's do not extend as far into the fluid as in the $\chi_{AS} = 0$ case. The A density around the B core is higher and it decays more rapidly away from the B domain than for the $\chi_{AS} = 0$ example. In fact, at $\chi_{AS} = 1.0$ and large surface separations, the micelles on each surface resemble "onionlike" structures,[17,18] with a B core and a thin, dense shell of A, as can be seen in Figure 4a. Again, this outer A layer shields the B component from the unfavorable solvent.

Figure 4b,c reveals the conformations of the chains as the surfaces are brought closer together for the $\chi_{AS} = 1.0$ example. As the layers are compressed, the B cores from the two surfaces merge into a single domain. (Again, the merging of the micelles happens at a distance that is greater than the vertical extent of the isolated micelles.) Now, however, the solvophobic A's are also driven to mutually associate and thereby shield themselves from the unfavorable solvent. The additional attraction between the A's results in a greater attraction between the surfaces, as can be seen in the plot of F_{int} versus L in Figure 3c. The minimum of the curve is lower than for $\chi_{AS} = 0$ and $\chi_{AS} = 0.5$. In addition, the minimum of the curve is shifted to smaller surface separations. Since the A component forms a thin shell, there is less resistance to the compression of the layers. When the compression is sufficiently large that distance between the surfaces is comparable to the size of the central "onion", the density of the A component starts increasing and the interaction between the layers becomes repulsive.

Effect of Increasing χ_{AB}; $\chi_{BS} = 2$. Up to this point, we have only considered compatible chains i.e., $\chi_{AB} = 0$. If the chains are relatively incompatible, the more soluble A chains are less able to shield the B component from the solvent. The shielding is now determined by the competition between the enthalpic gain due to the reduction in B−solvent contacts and the enthalpic loss due to the energetically unfavorable A−B contacts. If $\chi_{AB} = 0.5$, there is still a tendency for the more soluble component to shield the solvent-incompatible B. If, however, χ_{AB} is increased to 1.5, the shielding behavior is significantly diminished. Figure 5a shows the conformation of the layers for a fixed surface separation of $L = 9$ with $\chi_{AB} = 1.5$ and $\chi_{AS} = 0$. When the A chains are in a good solvent and the surfaces are far apart, the A's form a stretched brush (with a depletion in the region where the B micelles are located). Compression of the surfaces again leads to the merging of the B micelles for the same reasons as for $\chi_{AB} = 0$. Now, however, the A chains do not encircle the B cores, but rather, spread out uniformly in the region between the two surfaces. If the surfaces are compressed further, the density of the soluble component gradually increases. The situation is qualitatively similar for $\chi_{AS} = 0.5$.

In Figure 5b, χ_{AB} is again equal to 1.5; however, χ_{AS} is increased to 1 so that both chains are in poor solvents. Note that the onionlike structures seen in Figure 4a (for $\chi_{AS} = 1$ and $\chi_{AB} = 0$) do not appear if $\chi_{AB} = 1.5$. Instead, both A and B chains form their own micelles, which are

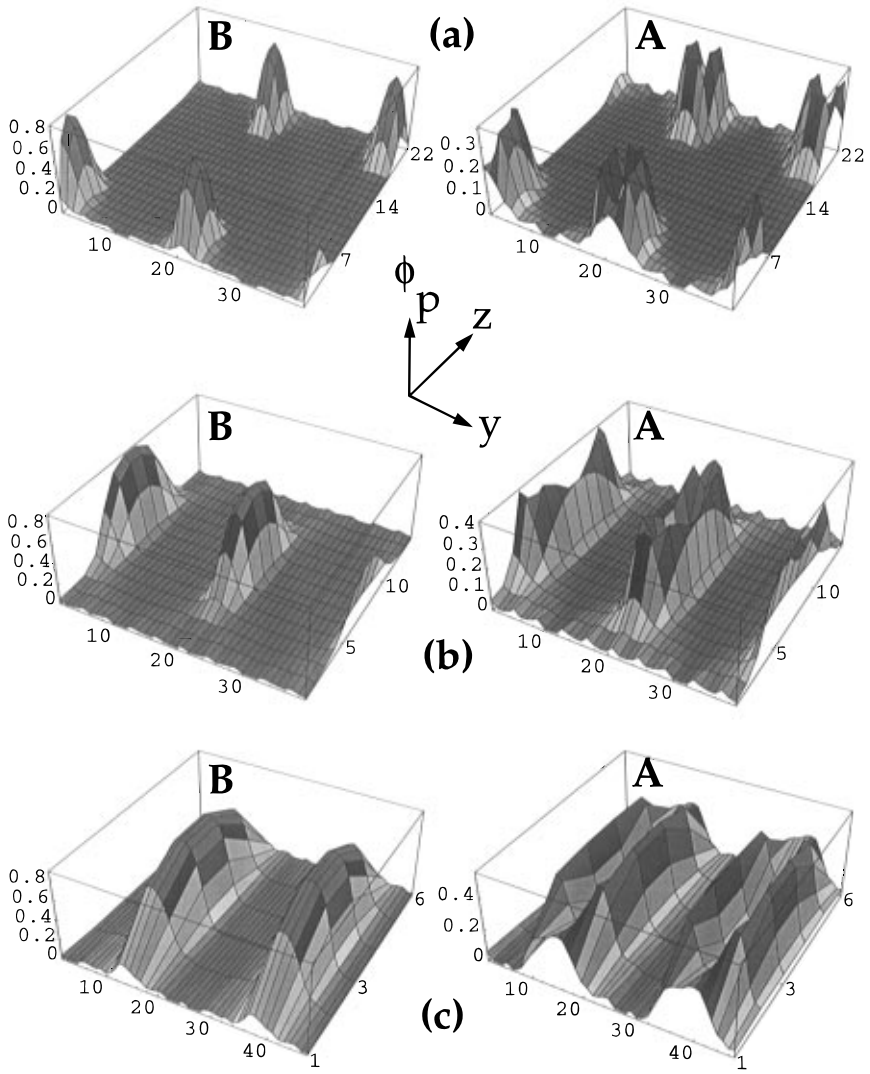

Figure 4. Plots showing the effect of decreasing the surface separation, L, for alternately grafted A−B chains where $N_A = N_B = 80$. The grafting density per line ρ is 0.025, $\chi_{Bs} = 2$, $\chi_{As} = 1$, and $\chi_{AB} = 0$. The figures are for the following surface separations: (a) $L = 21$, (b) $L = 13$, and (c) $L = 5$. Y refers to the grafting direction and ϕ_p denotes the polymer density. The plots marked "B" show the polymer density of the B blocks, while the plots marked "A" show the density of the A blocks.

adjacent to each other. There is little solvent at the boundaries between the two types of micelles. Since $\chi_{AS} < \chi_{BS}$, the density of the A core is lower than that of the B. Compression of the surfaces leads to the merging of the micelles from the opposite surfaces so that merged micelles of each type are formed in the center (see Figure 5b). The B micelles are more localized in the Z direction than the A micelles since localization reduces the area in contact with the solvent. Further compression of the surfaces does not change the core density of either of the micelles unless the distance between the surfaces is equal to or smaller than the size of the micelles.

The free energy of interaction as a function of surface separation for $\chi_{AB} = 0.5$ and 1.5 are also shown in Figure 3. The qualitative features in the cases of $\chi_{AB} > 0$ are very similar to those for $\chi_{AB} = 0$, including the presence of an attractive region ($F_{int} < 0$). In Figures 3a ($\chi_{AS} = 0$) and 3b ($\chi_{AS} = 0.5$), the strength of attraction decreases and the size of the attractive region shrinks as χ_{AB} increases. This is due to the extra enthalpic losses that arise from the A−B repulsion.

In Figure 3c, the A component is also solvophobic ($\chi_{AS} = 1.0$) and the energy of interaction is less sensitive to the value of χ_{AB} than if A is in a good or Θ solvent. Nonetheless, the surfaces are more attractive for $\chi_{AB} = 0$ than for $\chi_{AB} = 0.5$ (at a given surface separation); then, there is a change in the trend and the attraction is largest for $\chi_{AB} = 1.5$. Although the differences in F_{int} are very small for all three χ_{AB}'s in Figure 3c, the change in the trend can be attributed to the fact that the self-assembled structures are fundamentally different for $\chi_{AB} = 0$ and $\chi_{AB} = 1.5$. While for $\chi_{AB} = 0$ (and 0.5), the A chains shield the B component, separate micelles are formed by each component when $\chi_{AB} = 1.5$ (Figure 5b). And these micelles are driven to associate with their partners on the opposite surface, a behavior that increases the attraction between the surfaces.

Alternatively Grafted A and B Chains of Unequal Lengths. To determine if the interaction between the layers can be tailored by varying the relative chain lengths, we let the more soluble A component be twice as long ($N_A = 80$) as the less soluble B component ($N_B = 40$). Since the area of the micellar core is smaller here than in the cases above (where $N_B = 80$), smaller amounts of the more soluble polymer are needed to shield the B domain and the rest of the soluble polymer forms a stretched brush in a good or Θ solvent. The lower volume fraction of the B component shrinks the attractive region in the free energy of interaction, as can be seen in Figure 6. Comparison of Figures 3a and 6a shows that although the qualitative features as a function of surface separation are very similar, the initial repulsive region (before the micelles from the two

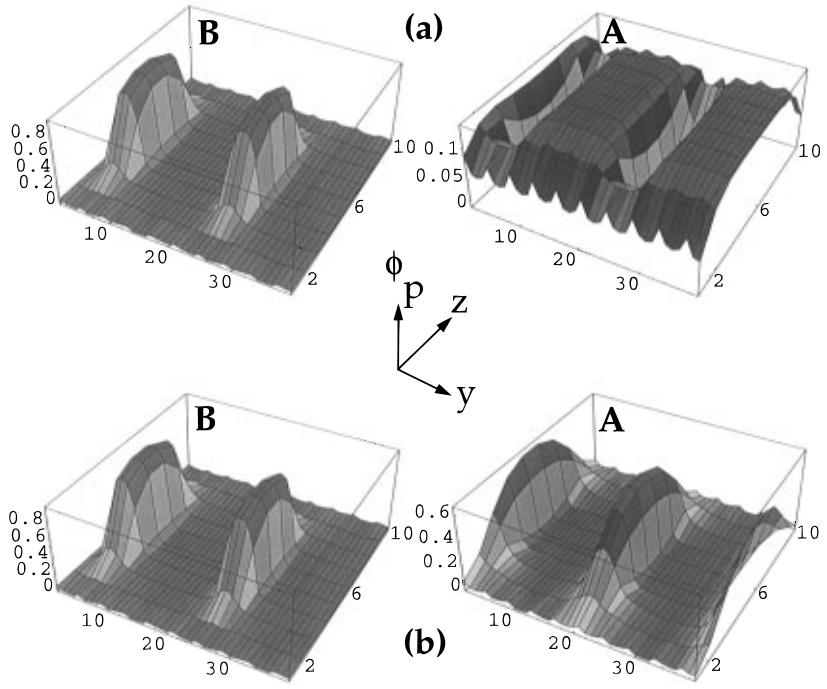

Figure 5. Plots showing the self-assembly for surface separation, $L = 9$, for alternately grafted A−B chains. The grafting density per line ρ is 0.025, $\chi_{Bs} = 2$, and $\chi_{AB} = 1.5$. The A−solvent interaction is (a) $\chi_{As} = 0$ and (b) $\chi_{As} = 1$. Y refers to the grafting direction and ϕ_p denotes the polymer density. The plots marked "B" show the polymer density of the B blocks, while the plots marked "A" show the density of the A blocks.

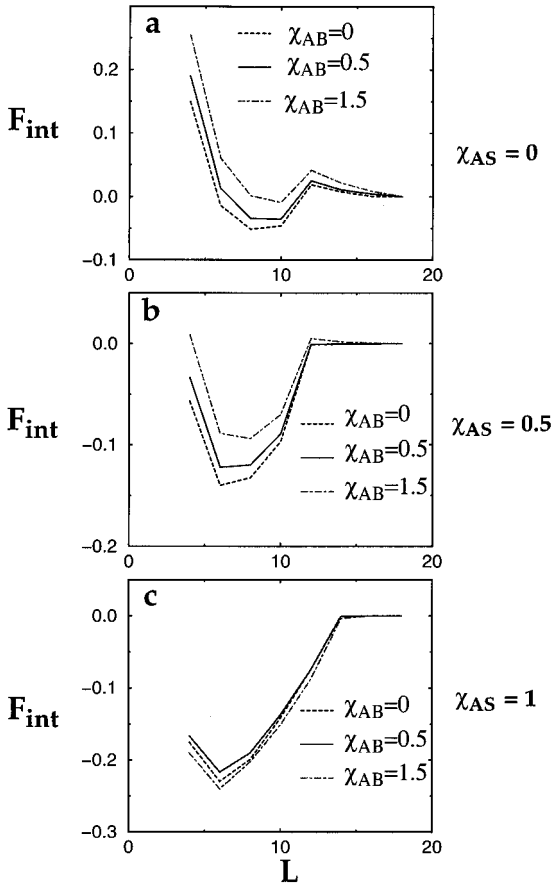

Figure 6. Free energy of interaction F_{int} as a function of surface separation, L, for alternately grafted A−B chains with $N_A = 80$ and $N_B = 40$. The grafting density per line ρ is 0.025 and $\chi_{Bs} = 2$. The A−solvent interaction is (a) $\chi_{As} = 0$, (b) $\chi_{As} = 0.5$, and (c) $\chi_{As} = 1$. Each of the figures shows results for three different χ_{AB}, which are shown with different types of lines.

surfaces merge) is more pronounced in Figure 6a than in Figure 3a. Moreover, if we compare the figures for the same values of χ_{AS}, the minima are lower in Figure 3 than in each of the corresponding cases in Figure 6. These curves indicate that the depth of the curves can be controlled by manipulating the length of the solvophobic chain. We return to this point below.

If we introduce a repulsive interaction between the two components by making $\chi_{AB} > 0$, the qualitative changes are similar to those for chains with equal length. This is clear from the plots in Figure 6 for $\chi_{AB} = 0.5$ and 1.5.

Compressing Surfaces Coated with Homopolymers of Different Solvent Affinities. Effect of Varying χ_{AS}; $\chi_{BS} = 2$, $\chi_{AB} = 0$. Another means of controlling the interaction between surfaces is to coat one substrate with homopolymer A and the other with homopolymer B, where again A and B have different solvent affinities. When the surfaces are far apart, the grafted homopolymers that are in a good or Θ solvent form stretched brushes, while those in a poor solvent form pinned micelles. Figure 7 shows the effects of bringing the surfaces together when one surface is covered with $\chi_{BS} = 2$ homopolymers and the other surface is coated with $\chi_{AS} = 0$ chains. As the surfaces start interacting (Figure 7a,b), there is an increase in the density of the soluble A component around the B micelles. This shields the solvophobic B's from the unfavorable solvent and thereby lowers the surface tension in the system. As the surfaces get closer, the shielding of the B chains by the soluble A component becomes more effective. Soon the morphology of the layers resembles the "flowerlike" structure described above (see Figure 2a). We note that the decrease in the surface separation causes the overall density of the soluble component to gradually increase since more and more of the solvent gets squeezed out of the system. However, the density of the B core remains relatively unchanged.

The increased shielding due to solvent expulsion leads to an enthalpic gain in the free energy, while the surface confinement results in entropic losses. This competition

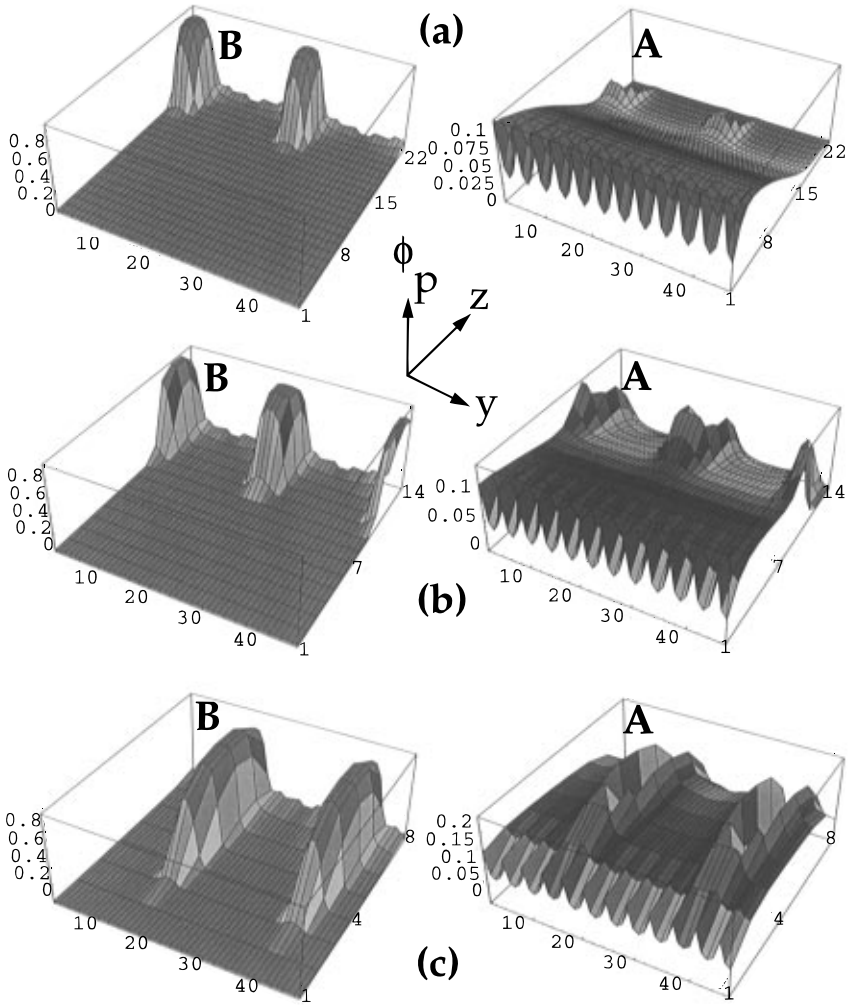

Figure 7. Plots showing the effect of decreasing the surface separation, L, when surfaces coated with homopolymers of different solvent qualities are compressed: (a) $L = 21$, (b) $L = 13$, and (c) $L = 7$. The length of both types of homopolymers is 80, the grafting density per line ρ is 0.025, $\chi_{Bs} = 2$, $\chi_{As} = 0$, and $\chi_{AB} = 0$. Y refers to the grafting direction and ϕ_p denotes the polymer density. The plots marked "B" show the polymer density of the B blocks, while the plots marked "A" show the density of the A blocks.

between the enthalpic and entropic free energies results in a net cancellation of the two effects. Therefore, the free energy of interaction plotted in Figure 8a appears to be relatively flat over a wide range of surface separations, even though the layers actually start interacting near $L \sim 20$ (as shown in Figure 7a). For $\chi_{AB} = 0$, however, the free energy of interaction has a small attractive region where the gain in enthalpy due to better shielding of the B component wins over the losses in the entropy due to the compression of surfaces. After this small attractive region, further compression of the surfaces leads to considerable entropic losses and the interaction profile becomes increasingly repulsive.

We note that if we compress a homopolymer surface with $\chi_{BS} = 2$ with an A layer that is not in a good solvent but in a Θ solvent ($\chi_{AS} = 0.5$), the features are qualitatively similar to those described above for the good solvent case. In the Θ solvent, however, the brush height is smaller and the brush density is higher because it is not as energetically favorable for the chains to stretch into the Θ solvent. Moreover, since the gain in the free energy in forming a highly stretched brush is less in a Θ solvent than in a good solvent, a much better shielding of the B component is obtained in the Θ solvent for the same surface separation. Thus, in a Θ solvent the enthalpic gains due to the shielding of the B chains outweigh the entropic losses due to confinement over a wider range of surface separations than for $\chi_{AS} = 0$. This can be seen in Figure 8b, which shows a very distinct minimum for $\chi_{AB} = 0$.

Figure 9 shows the effects of bringing together two surfaces that are both covered with homopolymers in poor solvents; for one, $\chi_{BS} = 2$, and for the other, $\chi_{AS} = 1$. When the layers are far apart, the chains form pinned micelles on both surfaces. As the surfaces come together, some of the A chains stretch toward the B surface to shield the more solvophobic component, while the remaining A chains still form pinned micelles near the grafting surface, as shown in Figure 9a. With further compression of the surfaces, all of the A chains stretch out to form "onionlike" shells around the B component. As the surfaces are brought closer together, the density of the B core and the outer A layer remain unchanged (Figure 9c). Eventually, when the surface separation becomes comparable to the vertical extent of the onion shell, the density of the A layer increases. The free energy of interaction in Figure 8c shows a much more pronounced attractive region in this case (compared to parts a and b of Figure 8) due to a greater enthalpic gain in this system. Of course, when the surfaces are highly compressed, entropic losses will eventually dominate and the interaction becomes repulsive.

Effect of Increasing χ_{AB}; $\chi_{Bs} = 2$. The effect of introducing a repulsion between the two homopolymers when A is in a good or Θ solvent is very similar to that

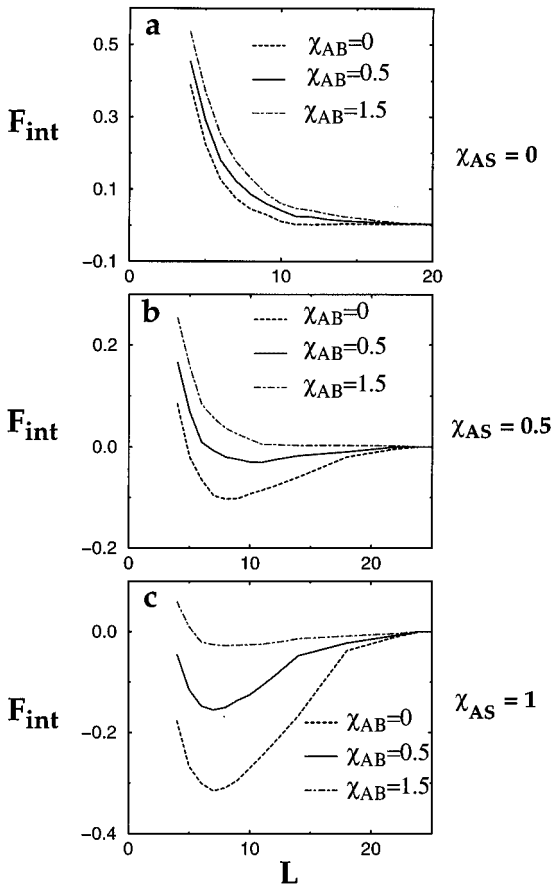

Figure 8. Free energy of interaction F_{int} as a function of surface separation, L, when surfaces coated with homopolymers of different solvent qualities are compressed. The length of both types of homopolymers is 80, the grafting density per line ρ is 0.025, and $\chi_{Bs} = 2$. The A−solvent interaction is (a) $\chi_{As} = 0$, (b) $\chi_{As} = 0.5$, and (c) $\chi_{As} = 1$. Each of the figures shows results for three different χ_{AB}, which are shown with different types of lines.

described above. The shielding of the B component by the A chains, which form a stretched brush, gradually decreases as χ_{AB} increases. For $\chi_{AB} = 1.5$, there is very little shielding left. As the surfaces are compressed, the density of the homopolymer brush increases monotonically (except for the presence of depletion regions, where the B micelles are located).

The structural changes in the presence of $\chi_{AB} > 0$ are more pronounced when both components are in poor solvents. Figure 10 shows the changes in the self-assembly of the layers when $\chi_{BS} = 2$, $\chi_{AS} = 1$, and $\chi_{AB} = 1.5$. As the surfaces are brought together, the micelles formed near both the surfaces start overlapping to some extent. With further compression of the surfaces, the micelles formed by the A chains attempt to shield the B micelles, as shown in Figure 10b. In particular, the micelles formed by the A chains split into two and shield both sides of the B micelles. If the separation between the surfaces becomes smaller than the size of the micelles, the size of the A micelles increases laterally although their core density does not change noticeably. In the highly compressed state, two of the A micelles, which shield two adjacent B micelles, merge so that the chains form alternate A and B micelles between the surfaces (Figure 10c).

The free energy of interaction as a function of surface separation for $\chi_{AB} = 0.5$ and 1.5 are shown in Figure 8 along with $\chi_{AB} = 0$. Again, the attractive region shrinks and for the same surface separation, the interaction becomes less attractive as χ_{AB} increases.

Scaling Model and Results

The interaction energies we calculate for polymer-coated surfaces can be classified into four qualitatively distinct classes, as in Figure 11. In the first of these, the interaction energy is *micelle-dominated*. In Figure 3, the interaction energy nearly vanishes for plate separations greater than $L = 18$. When the separation is lowered to $L = 18$, the micelles from each surface merge and form a large central core located in the gap between the plates. The micelle forces the plates toward $L = 0$. However, when the separation becomes too small, the soluble A chains are compressed, causing the eventual upturn in the interaction free energy for intermediate L. The second type of interaction is *brush-dominated*. In Figure 8a, the interaction potential is purely repulsive. The response of the system is dominated by the compression of the swollen A brush as the plates are brought together. The third type of interaction profile resembles a *ratchet*. As in Figure 6a, there is an initial repulsion between the surfaces, followed by a large attractive region and then further repulsion. If the surfaces are driven together with sufficient force to overcome the initial repulsion, they bind at the global minimum of the interaction. The fourth type of profile is hinted at in the upper curve in Figure 6a. Here, the minimum is barely attractive. With a slight increase in χ_{AB}, the global minimum near $L = 10$ becomes a local minimum. (The true global minimum of the interaction is at large plate separations.) In this case, there is a *metastable* equilibrium point in the free energy profile.

These interaction types (micelle-dominated, brush-dominated, ratcheting, and metastable) have different implications for controlling a solution of coated particles. Brush-dominated interactions stabilize the dispersion, while micelle-dominated interactions promote aggregation into clusters characterized by a well-defined, nonzero separation. Ratcheting interactions also promote aggregation with a well-defined separation. However, the initial repulsion has an effect on the kinetics of aggregation. A metastable interaction provides steric stabilization like that given in the brush-dominated regime. However, in thermodynamic equilibrium, there is a band of inaccessible particle separations near the kink in the free energy. (We produce a properly concave interaction free energy by employing a Maxwell construction, as indicated by the dashed lines in Figure 11.)

To study these interaction types, we employ a simple model.[9−12,19,20] Each surface is coated with A and B homopolymers, with an area per chain of s_A for the A chains and s_B for the B chains. The A chains have N_A monomers, and the B chains have N_B monomers. We assume that the solvent is athermal for A, but poor for B. We define a solvent quality parameter $\tau = (2\chi - 1)/2\chi$, where $\chi > {}^1/_2$ is the Flory−Huggins mixing parameter for B monomers and the solvent. We assume that $\chi_{AB} = \chi$, so that there is no shielding effect to consider. We could relax this condition in a more detailed treatment, but for now this simplification helps to clarify the analysis. Finally, we assume that monomers interact with the surfaces through Flory−Huggins parameters $\chi_{AW} = 0$ and $\chi_{BW} = \chi$. Thus, the surface is nonadsorbing for both A and B.

At large separations, the B homopolymers form pinned micelles that coat the surfaces, and we assume that N_A and s_A are such that the A polymers form brushes. The situation is akin to that depicted in Figure 2a. (The important difference between the system pictured in Figure 2a and the one we consider here is that the A polymer does not shield the B cores.) We

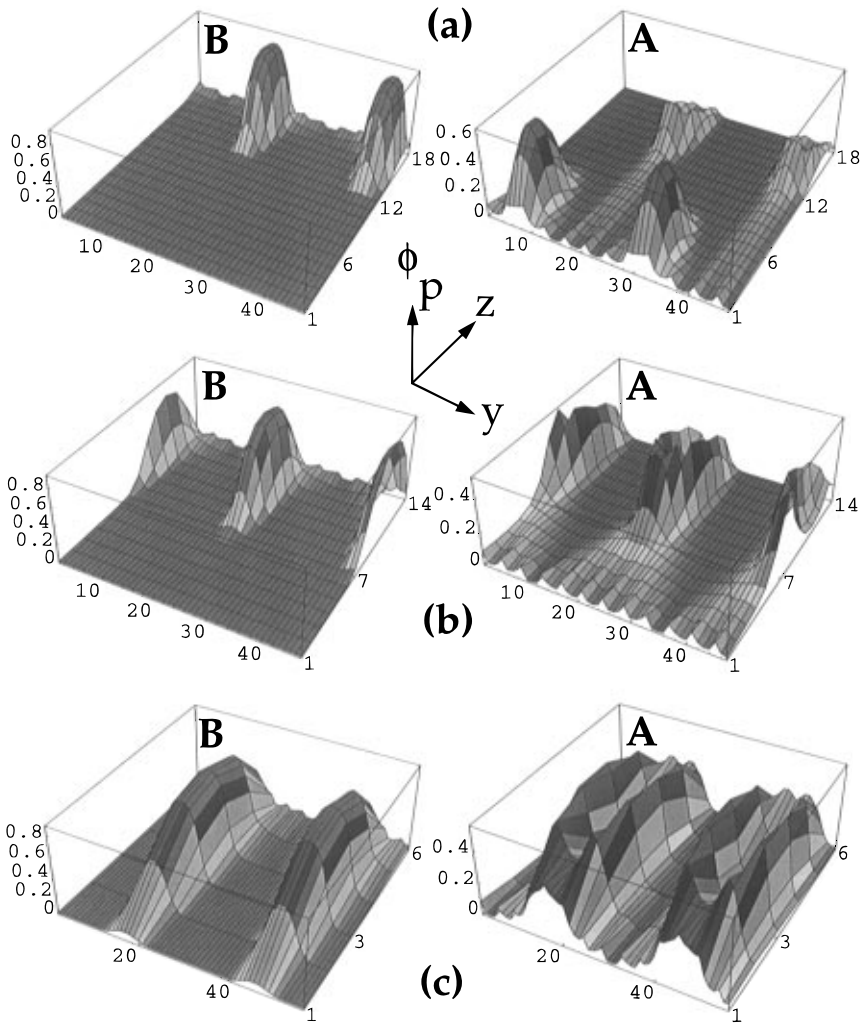

Figure 9. Plots showing the effect of decreasing the surface separation, L, when surfaces coated with homopolymers of different solvent qualities are compressed: (a) $L = 17$, (b) $L = 13$, and (c) $L = 5$. The length of both types of homopolymers is 80, the grafting density per line ρ is 0.025, $\chi_{Bs} = 2$, $\chi_{As} = 1$, and $\chi_{AB} = 0$. Y refers to the grafting direction and ϕ_p denotes the polymer density. The plots marked "B" show the polymer density of the B blocks, while the plots marked "A" show the density of the A blocks.

treat the A and B systems independently, as is justified in the absence of shielding and when the typical distance between adjacent micelles is large. We define H such that the plate separation, L, is given by $L = 2H$.

For simplicity, we employ the Alexander and de-Gennes approximation for the A brush; that is, we assume that the free ends of the grafted chains are localized in a single plane parallel to the grafting surfaces.[19,20] When the surfaces are far apart, the free energy per chain in the brush is given by

$$F(H) = \frac{3}{2}\frac{H^2}{a^2 N_A} + \frac{a^3 {N_A}^2}{H s_A} \tag{8}$$

where H is the as yet unknown height of the unperturbed brush and a^3 is the effective volume per monomer. Minimizing $F(H)$ with respect to H yields

$$H_{br} = 3^{-1/3} a^{5/3} {s_A}^{-1/3} N_A \tag{9}$$

and

$$F^0_{br} = (3^{4/3}/2) a^{4/3} {s_A}^{-2/3} N_A \tag{10}$$

where H_{br} is the undisturbed thickness of the brush and F^0_{br} is the free energy per chain in the brush. Then, the interaction free energy of the brush per chain (as defined above) is

$$\Delta F_{br} = \begin{Bmatrix} 0 & \text{when } H \geq H_{br} \\ F^0_{br}\, g\left(\dfrac{H}{H_{br}}\right) & \text{when } H \leq H_{br} \end{Bmatrix} \tag{11}$$

where

$$g\left(\frac{H}{H_{br}}\right) = \frac{F(H/H_{br})}{F^0_{br}} - 1 = \frac{1}{3}(H/H_{br})^2 + \frac{2}{3}(H_{br}/H) - 1 \tag{12}$$

Note that $g(1) = 0$; $F^0_{br}\, g(x)$ is the difference in free energy between a compressed brush (with $x = H/H_{br} < 1$) and the uncompressed layer (where the brush thickness is equal to H_{br}). When $H > H_{br}$, the brushes are undisturbed, while if $H < H_{br}$, each brush is compressed at a cost in free energy.

The B system forms pinned micelles on each surface. At $H = H^*$, the B micelles merge to form micelles centered in the gap between the surfaces, with long stretched legs going from the micelle toward each surface. We first analyze the situation for separations with $H > H^*$, where the micelles are localized on the surface.[9−12] Each micelle is a sphere of radius R resting on the substrate, and f chains grafted over an area of $\pi D^2 = f s_B$ make up the micelle. The free energy per

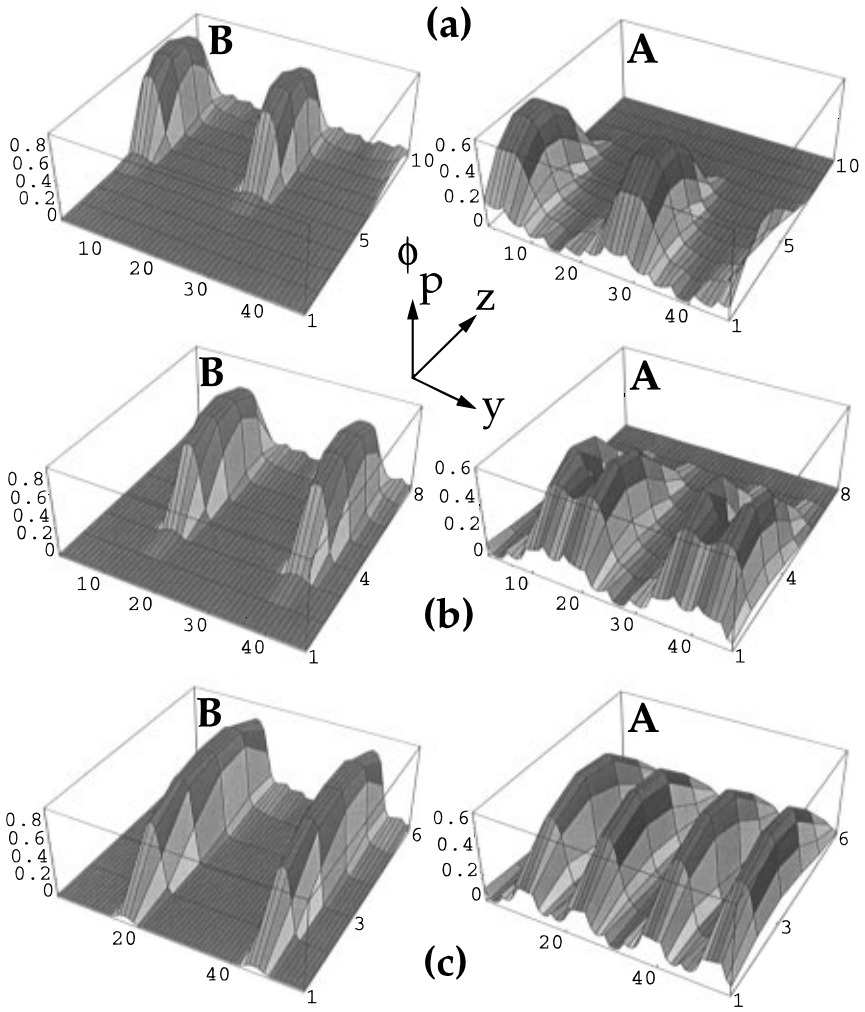

Figure 10. Plots showing the effect of decreasing the surface separation, L, when surfaces coated with homopolymers of different solvent qualities are compressed: (a) $L = 9$, (b) $L = 7$, and (c) $L = 5$. The length of both types of homopolymers is 80, the grafting density per line ρ is 0.025, $\chi_{Bs} = 2$, $\chi_{As} = 1$, and $\chi_{AB} = 1.5$. Y refers to the grafting direction and ϕ_p denotes the polymer density. The plots marked "B" show the polymer density of the B blocks, while the plots marked "A" show the density of the A blocks.

chain in this conformation is[9−12]

$$F = 4\pi\gamma R^2/f + D/\xi \tag{13}$$

where the blob size, ξ, is equal to a/τ for small τ (we assume throughout that $D \gg R$).[21] The surface energy γ may be estimated as $\gamma = 1/\xi^2$. The first term is the surface energy per chain due to the interface between the micellar core and solvent, and the second is the stretching energy per leg or, equivalently, the number of thermal blobs per stretched leg. Since the core consists of close-packed blobs, we have that

$$R^3 = \frac{N_B}{n_B}\xi^3 f \rightarrow R^3 = fN_B a^3 \tau^{-1} \tag{14}$$

where $n_B = \xi^2/a^2$ is the number of monomers per thermal blob. Thus, the free energy per chain can be expressed as a function of N_B, s_B, τ, a, and R. Minimizing the free energy with respect to R determines the equilibrium structure of the pinned micelle:

$$D_{pm} = \left(\frac{2}{3}\right)^{3/5} \pi^{-1/5} a^{3/5} \tau^{1/5} s_B{}^{1/5} N_B{}^{2/5} \tag{15}$$

and

$$F_{pm} = 5(108\pi)^{-1/5} a^{-2/5} \tau^{6/5} s_B{}^{1/5} N_B{}^{2/5} \tag{16}$$

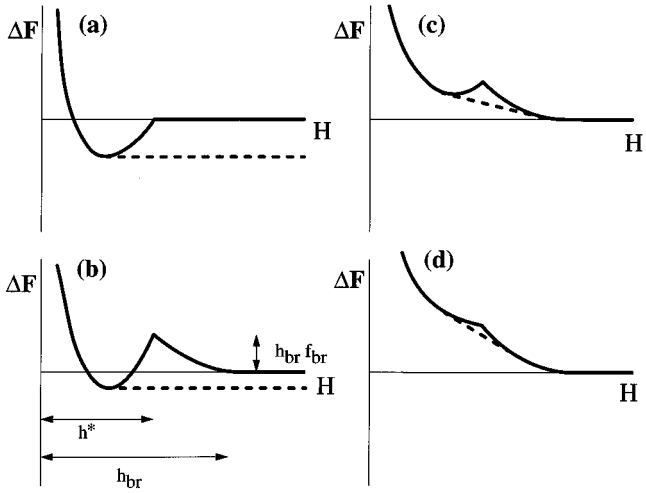

Figure 11. Interaction types. (a) Micelle dominated. The thermodynamic phases are $H = H_{min}$ and $H \rightarrow \infty$. The dotted line is produced by a Maxwell construction. (b) Ratchet. The thermodynamic phases are as in part a, but the adjustable repulsive tail has implications for the kinetics of aggregation. (c) Metastable. The interaction is generally repulsive, but near the local minimum there is a band (via the Maxwell construction) of unstable particle separations. (d) Brush dominated. There is no longer a local minimum in the interaction profile, and the unstable band is small.

where D_{pm} is the lateral extent of the equilibrium structure and F_{pm} is the free energy per chain in the

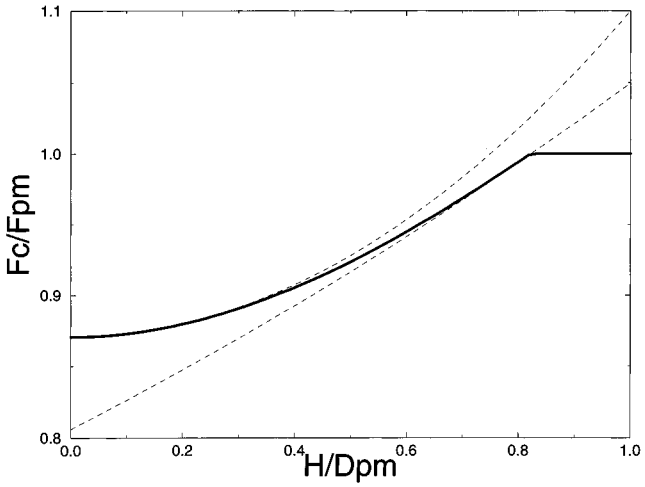

Figure 12. The pinned micelle free energy. The bold curve indicates the free energy as a function of H/D_{pm} of the pinned micelle system. For $H/D_{pm} > 0.823$, the system forms noninteracting pinned micelles on each surface. The dashed lines indicate expansions around $H = 0$ and $H = D_{pm}$ that are used to interpolate the bold curve.

pinned micelle state.

The pinned micelle may also form in the gap between the surfaces. Then, the free energy per chain has the form

$$F = 4\pi\gamma R^2/(2f) + (D^2 + H^2)^{1/2}/\xi \qquad (17)$$

The surface energy per chain is lowered by a factor of 2, since the common micelle is made of $2f$ chains, f coming from each surface. Following the calculation outlined above and expanding eq 17 for small H (again, with the understanding that $R \ll H$), the H-dependent free energy of the centered micelle is[22]

$$F_c = F_{pm}\left(2^{-1/5} + \frac{2^{1/5}}{5}\frac{H^2}{D_{pm}^2}\right) + O\left[\frac{H}{D_{pm}}\right]^3 \qquad (18)$$

For $H \ll D_{pm}$, the free energy per chain is lower than the state where the micelles are formed separately on the walls, but the free energy rises as the stretching is increased by an increase of H. Eventually, the centered micelles divide into two and jump to each surface, at which point the free energy per chain becomes constant in H. The transition occurs near $H/D_{pm} \approx O[1]$. The transition point may be analyzed by expanding eq 17 about $D = D_{pm}$ and $H = D_{pm}$ to the second order. From this expression, we find that the jumping transition occurs at $H^* = 0.823D_{pm}$. We approximate $F_c(H)$ for $H < H^*$ by a quintic polynomial that matches the expansions for small H and for H near D_{pm}. $F_c(H)$ is shown in Figure 12, with a comparison to the expansions for $H \ll D_{pm}$ and $H/D_{pm} \approx$ O[1]. We define $\Delta F_c = F_c(H) - F_{pm}$. The total interaction free energy, ΔF, is defined by

$$\Delta F = \Delta F_{br} + \Delta F_c \qquad (19)$$

$\Delta F(H)$ differs from F_{int} above in that ΔF is a free energy per chain, while F_{int} is loosely the free energy per unit area.

ΔF can be classified into one of the above four categories, as demonstrated in Figure 13. We define two parameters: $f_{br} = F_{br}/F_{pm}$, and $h_{br} = H_{br}/D_{pm}$. When $h_{br} < h^* = 0.823$, the potential is micelle-dominated. This corresponds to region **A**. The micelles merge before the brushes come into contact, so that there is always an attractive region (not preceded by an initial repulsion). When $h_{br} > h^*$, the behavior of the potential is controlled by f_{br}. For large f_{br}, the potential is purely repulsive, but there is a kink in the free energy near $H = H^*$. This is region **D**. As f_{br} is decreased, a local minimum appears in the potential (region **C**), and if f_{br} is decreased even further, this local minimum becomes the true global minimum (region **B**). The boundary between regions **D** and **C** and the boundary between regions **B** and **C** are asymptotically of the form $f_{br} \sim h_{br}^{-1}$ in the limit $h_{br} \gg 1$.

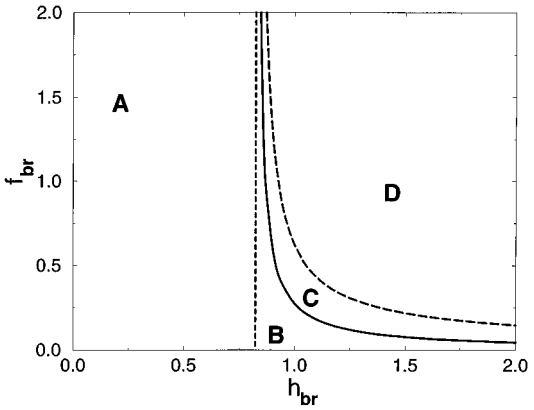

Figure 13. Diagram of interaction types. (a) Micelle-dominated interactions. Here the coalescence of the micelles dominates the free energy of interaction. There is a single global minimum and no initial repulsion in the interaction free energy. (b) Ratcheting interactions. Here the interaction free energy has an initial repulsion that shields the global minimum. (c) Metastable interactions. There is a cusp in the free energy, followed by a local minimum. The free energy is repulsive and provides steric stabilization. (d) Brush dominated. The free energy is purely repulsive, although there is a cusp in the interaction when the micelles merge.

The region corresponding to the ratcheting potential (region **B**) is the most interesting, and we deduce a number of properties of the interaction in this region (qualitatively shown in Figure 11b). First, the range of the initial repulsion is given by the unperturbed brush height, $H = H_{br} > H^*$. The cusp occurs when the micelle jumps to the gap between the surfaces at $H = H^*$. The free energy barrier that must be overcome to reach the global minimum is proportional to $f_{br}h_{br}$. Since adjusting N_A and s_A provides independent control over f_{br} and h_{br}, by tailoring N_A and s_A we can in principle choose the interaction type from among the above four. Additionally, when the interaction is of the ratcheting type, control over the range and free energy barrier of the interaction can be gained by correctly designing the coverage and molecular weight of the soluble component. This fine level of control is relatively easy to achieve, low in cost to implement, and of enormous practical use in designing tunable colloidal dispersions for specific applications.

Conclusions

We calculated the interaction between surfaces that are coated with a binary mixture of A *and* B homopolymers and between surfaces that are covered with A *or* B chains. At least one of the polymers is in a poor solvent. The chains are grafted at low densities and form such self-assembled structures as "onionlike" and "flowerlike" micelles. We found that the free energy of interaction has a large attractive region even if one of the components is in a good or Θ solvent. In the case of alternately grafted A and B chains, this behavior is observed even when the solvophilic component is twice

as long as the solvophobic chains and, thus, makes the first contact with the opposing surface.

The attraction between the surfaces is due to the formation of novel self-assembled structures as the surfaces are brought into contact. Note that the formation of pinned micelles, and the self-assembly between the layers, only occurs at low grafting densities. Thus, the behavior observed in these studies is in sharp contrast to the behavior of the system at high grafting densities, where the chains form dense brushes and the surfaces exhibit a monotonic repulsion.[7]

Our findings provide guidelines for controlling the interactions between polymer-coated substrates in solution. The results reveal that specified interactions can be obtained by grafting a low volume fraction of solvophobic (B) and solvophilic (A) chains and tailoring the A−solvent or A−B energies or the relative lengths and coverages of the different homopolymers.

Acknowledgment. We thank Drs. Ekaterina Zhulina, Dilip Gersappe, and Prof. David Jasnow for helpful discussions. This work was supported in part by ONR grant N00014-91-J-1363, NSF grant DMR-9407100, and DOE grant DE-FG02-90ER45438 to A.C.B. and NSF grant DMR-92-17935 to D. Jasnow.

References and Notes

(1) Klein, J.; Kamiyama, Y.; Yoshizawa, H.; Israelachvili, J. H.; Fredrickson, G. H.; Pincus, P.; Fetters, L. J. *Macromolecules* **1993**, *26*, 5552.
(2) Klein, J.; Perahia, D.; Warburg, S. *Nature* **1991**, *352*, 143.
(3) (a) Taunton, J.; Toprakcioglu, C.; Fetters, L. J.; Klein, J. *Nature* **1988**, *332*, 712. (b) Taunton, J.; Toprakcioglu, C.; Fetters, L. J.; Klein, J. *Macromolecules* **1990**, *23*, 571.
(4) Hadziannou, G.; Patel, S.; Granick, S.; Tirrell, M. *J. Am. Chem. Soc.* **1986**, *108*, 2869.
(5) Patel, S.; Tirrell, M. *Annu. Rev. Phys. Chem.* **1989**, *40*, 597.
(6) Israelachvili, J. N.; Tandon, R. K.; White, L. R. *Nature* **1977**, *277*, 120.
(7) Chen, C.; Dan, N.; Dhoot, S.; Tirrell, M.; Mays, J.; Watanabe, W. *Israel J. Chem.* **1995**, *35*, 41.
(8) Singh, C.; Balazs, A. C. *J. Chem. Phys.* **1996**, *105*, 706.
(9) Singh, C.; Zhulina, E. B.; Gersappe, D.; Pickett, G. T.; Balazs, A. C. A "Jumping Micelle" Phase Transition. *Macromolecules*, in press.
(10) Klushin, L. I., unpublished work.
(11) Williams, D. R. M. *J. Physique II* **1993**, *3*, 1313.
(12) (a) Zhulina, E. B.; Borisov, O. V.; Pryamitsyn, V. A.; Birshtein, T. M. *Macromolecules* **1991**, *24*, 140. (b) Zhulina, E. B.; Borisov, O. V.; Pryamitsyn, V. A. *J. Colloid Interface Sci.* **1990**, *137*, 295. (c) Zhulina, E. B.; Birshtein, T. M.; Pryamitsyn, V. A.; Klushin, L. I. *Macromolecules* **1995**, *28*, 8612.
(13) Yeung, C.; Balazs, A. C.; Jasnow, D. *Macromolecules* **1993**, *26*, 1914.
(14) Recall that, at high grafting densities, the solvophobic chains form a dense, collapsed layer, while the soluble chains form stretched brushes.
(15) Fleer, G.; Cohen-Stuart, M. A.; Scheutjens, J. M. H. M.; Cosgrove, T.; Vincent, B. *Polymers at Interfaces*; Chapman and Hall: London, 1993.
(16) (a) Huang, K.; Balazs, A. C. *Phys. Rev. Lett.* **1991**, *66*, 620. (b) Huang, K.; Balazs, A. C. *Macromolecules* **1993**, *26*, 4736. (c) Israels, R.; Gersappe, D.; Fasolka, M.; Roberts, V. A.; Balazs, A. C. *Macromolecules* **1994**, *27*, 6679.
(17) Zhulina, E. B.; Singh, C.; Balazs, A. C. Self-Assembly of Tethered Diblocks in Selective Solvents. *Macromolecules*, in press.
(18) Zhulina, E. B.; Singh, C.; Balazs, A. C. *Macromolecules* **1996**, *29*, 6338−6348.
(19) Alexander, S. *J. Phys. (Paris)* **1977**, *38*, 983.
(20) deGennes, P.-G. *J. Phys. (Paris)* **1976**, *36*, 1443.
(21) Lifshitz, I. M.; Grossberg, A. Y.; Khokohlov, A. R. *Rev. Mod. Phys* **1978**, *50*, 683.
(22) The notation $0[x]$ means "on the order of x".

MA9608129